

# Quantitative comparison of dose distribution in radiotherapy plans using 2D gamma maps and X-ray computed tomography

Abdulhamid Chaikh<sup>1</sup>, Jacques Balosso<sup>1,2</sup>

<sup>1</sup>Department of Radiation Oncology and Medical Physics, University Hospital of Grenoble, Grenoble, France; <sup>2</sup>University of GrenobleAlpes Grenoble, France

*Correspondence to:* Abdulhamid Chaikh. Department of Radiation Oncology and Medical Physics, University Hospital of Grenoble, Grenoble, France. Email: abdulhamedc@yahoo.com.

**Background:** The advanced dose calculation algorithms implemented in treatment planning system (TPS) have remarkably improved the accuracy of dose calculation especially the modeling of electrons transport in the low density medium. The purpose of this study is to evaluate the use of 2D gamma ( $\gamma$ ) index to quantify and evaluate the impact of the calculation of electrons transport on dose distribution for lung radiotherapy.

**Methods:** X-ray computed tomography images were used to calculate the dose for twelve radiotherapy treatment plans. The doses were originally calculated with Modified Batho (MB) 1D density correction method, and recalculated with anisotropic analytical algorithm (AAA), using the same prescribed dose. Dose parameters derived from dose volume histograms (DVH) and target coverage indices were compared. To compare dose distribution, 2D  $\gamma$ -index was applied, ranging from 1%/1 mm to 6%/6 mm. The results were displayed using  $\gamma$ -maps in 2D. Correlation between DVH metrics and  $\gamma$  passing rates was tested using Spearman's rank test and Wilcoxon paired test to calculate P values.

**Results:** the plans generated with AAA predicted more heterogeneous dose distribution inside the target, with  $P < 0.05$ . However, MB overestimated the dose predicting more coverage of the target by the prescribed dose. The  $\gamma$  analysis showed that the difference between MB and AAA could reach up to  $\pm 10\%$ . The 2D  $\gamma$ -maps illustrated that AAA predicted more dose to organs at risks, as well as lower dose to the target compared to MB.

**Conclusions:** Taking into account of the electrons transport on radiotherapy plans showed a significant impact on delivered dose and dose distribution. When considering the AAA represent the true cumulative dose, a readjusting of the prescribed dose and an optimization to protect the organs at risks should be taken in consideration in order to obtain the better clinical outcome.

**Keywords:** Electrons transport; gamma maps; radiotherapy dosage; computed tomography; bootstrap

Submitted Apr 12, 2016. Accepted for publication May 25, 2016.

doi: 10.21037/qims.2016.06.04

**View this article at:** <http://dx.doi.org/10.21037/qims.2016.06.04>

## Introduction

In radiotherapy the tumor control is directly correlated to the prescribed dose. The truly delivered dose is expected to be as close as possible to the prescribed dose. This depends on the accuracy and performance of the dose calculation algorithm which converts the prescribed dose into monitor units to perform the irradiation of the patient. Many years ago, the delivered dose was calculated considering homogeneous tissues densities equivalent to water,

whatever their real densities. The advanced dose calculation algorithms, integrated in treatment planning system (TPS), such as collapsed-cone convolution (CCC), anisotropic analytical algorithm (AAA), and more recently Acuros XB<sup>®</sup> have remarkably improved the accuracy of dose calculation, especially by taking fully account of real tissue density and by introducing more realistic electron transport models (1-7). These new algorithms have been rapidly integrated and used in the clinical practice of radiation oncology.

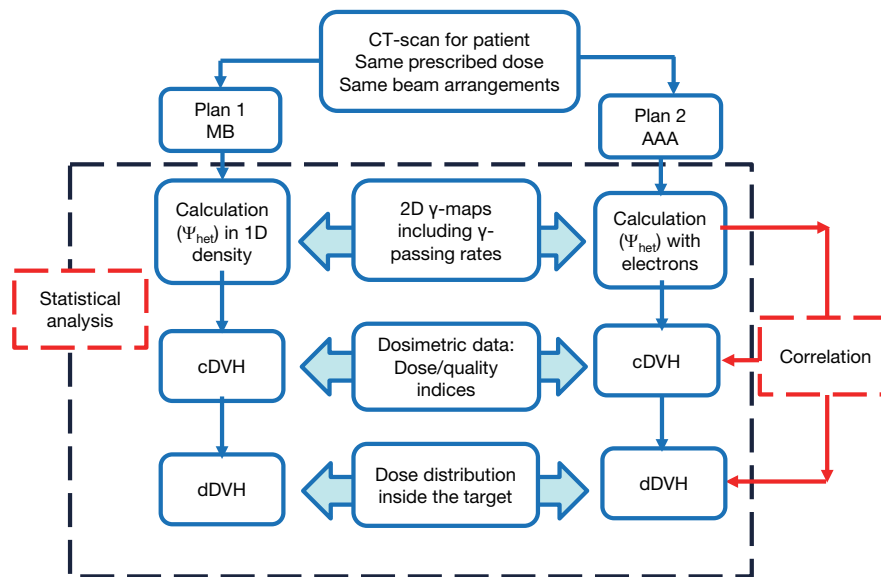


**Figure 1** Flowchart to compare radiotherapy plans, using  $\gamma$ -index. The fluency in the heterogeneity (het) was calculated using MB and AAA for each patient with the same CT-scan. MB, Modified Batho; AAA, anisotropic analytical algorithm.

However, a critical point is the discrepancy between these fast changing dosimetric methods regarding the long delay necessary to assess the clinical outcomes, in particular the benefits/risks balance. Risks could increase if we ignore the limits of this new generation of TPS, especially for thoracic irradiations due to the lung heterogeneity. The purpose of this paper is to illustrate a method to evaluate and quantify the consequences of the use of algorithms taking account of electrons transport on dose distribution calculated for lung, in one hand. In the other hand, to determine how dose volume histogram (DVH) metrics correlate with local difference in dose distribution using 2D gamma index ( $\gamma$ ). We have evaluated if the dose difference correlates with  $\gamma$  passing rates and if an adjustment of the prescribed dose is necessary to reproduce clinical results similar to those acquired with the former algorithms.

## Methods

### Treatment plans

This study is based on twelve radiotherapy treatment plans for lung cancer. A computed tomography (CT-scan) was carried out for each patient, then the images were loaded into Eclipse<sup>®</sup> TPS (Varian Medical Systems, Palo Alto, CA). The target volumes, including the security margins and the organs at risks, were delineated by the radiation oncologist. The treatments were performed with 18 MV photons. The

conventional radiation course varied from 50 to 66 Gy in fractions of 2 Gy. The plans were initially calculated with Modified Batho (MB) density correction method, and then recalculated with AAA using the same prescribed dose. MB does not model the change in lateral transport of electrons, but use the electron density information in one dimension (1D) along a ray path from the source to the point of interest (8-10). The dose distribution using AAA is obtained by the superposition of the doses from the photons and electrons convolutions (11,12).

### Evaluation of radiotherapy treatment plans

Figure 1 shows the flowchart of the comparison of dose calculation algorithms including 2D  $\gamma$ -maps, dosimetric and statistical analysis.

### Quantification of dose differences according to the 2D $\gamma$ -index

The impact of secondary electrons on heterogeneity correction was analyzed using the two dimensional (2D)  $\gamma$ -index by comparing the dose distributions from MB and AAA (13-15). The DICOM images were exported for each patient from TPS to RIT-113<sup>®</sup> (Dosimetry System Version 5.2, Radiological Imaging Technology, Inc., CO). The results were displayed using 2D  $\gamma$ -maps showing the pixels with  $\gamma$ -values greater than one, which were outside

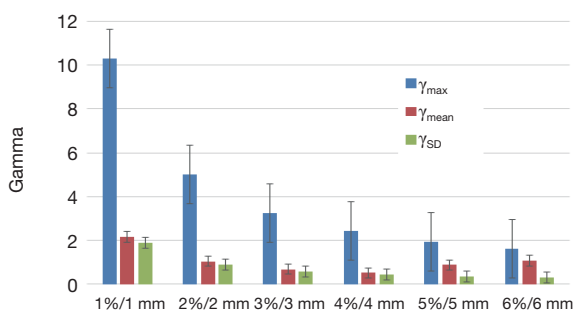


**Figure 2** Results of 2D gamma index including  $\gamma_{max}$ ,  $\gamma_{mean}$ , and  $\gamma_{SD}$  for all plans.

of tolerance range. In order to discriminate over/under-estimated dose, a color code was attributed to the dose difference ( $\Delta Dose$ ). Six criteria levels were applied and analyzed: 1%/1, 2%/2, 3%/3, 4%/4, 5%/5 and 6%/6 mm. For each criteria level, the results from 2D  $\gamma$ -index, including the  $\gamma$ -passing rates ( $\gamma_{rates}$ ) which are indicating the number of voxels with  $\gamma \leq 1$ , mean gamma ( $\gamma_{mean}$ ) with standard deviation ( $\gamma_{SD}$ ) and maximum gamma ( $\gamma_{max}$ ) were evaluated. The dose difference in percentage was calculated as:

$$\Delta Dose (\%) = (D_{AAA} - D_{MB}) \times 100 / D_{AAA} \quad [1]$$

### Dose volume histograms metrics

The dosimetric effects on the target coverage was firstly quantified using dosimetric parameters provided by the cumulative and differential dose volume histograms [cDVH, dDVH] for each radiotherapy plan. For each target the minimum dose ( $D_{min}$ ), mean dose ( $D_{mean}$ ), maximum dose ( $D_{max}$ ), as well as the calculated dose to 95% of the target volume ( $D_{95}$ ) were compared. In addition, the Coverage Index ( $C_{OI}$ ), Conformity Index for the target volume ( $CI_{TV}$ ) and S-index were calculated to determine the setup effects on dose distribution (16-18):

$C_{OI}$  = minimal isodose surrounding the TV/reference isodose

[2]

$$CI_{TV} = TV \text{ receiving } 95\% \text{ of the prescribed dose} / TV \quad [3]$$

$$S - index = \sqrt{\frac{\sum_{j=1}^{TV} [D(j) - D_{mean}]^2}{TV}} \quad [4]$$

where  $D(j)$  is the relative dose in the lesion voxel  $j$ ,  $D_{mean}$  is the average relative dose in the lesion and TV is the target

volume built of elementary voxels.

### Statistical analysis

The DVH metrics and the results from 2D  $\gamma$ -index were included in the analysis. A bootstrap simulation method with 1,000 random samplings was used to calculate the 95% confidence interval (95% CI) (19). The correlation coefficients ( $\rho$ ) from Spearman's rank correlation test were analyzed to assess inter-variable correlation between DVH metrics from MB and AAA, and  $\gamma$ -index with  $\Delta DVH$ . The Wilcoxon signed rank test was used to calculate the P value. A bilateral statistical test was carried out with an error  $\alpha=5\%$ , corresponding to 95% CI. The dose difference is considered significant when  $P < 0.05$ .

## Results

### 2D gamma maps

We observed that to satisfy the tolerance 95% of pixels with  $\gamma \leq 1$ , the criteria 6%/6 mm was needed at least. The Figure 2 shows the results of  $\gamma$  including  $\gamma_{mean}$ ,  $\gamma_{max}$  and  $\gamma_{SD}$  for all the sets of  $\gamma$  criteria. The Figure 3A shows the isodose curves calculated using MB and AAA and the Figure 3B shows an example of 2D  $\gamma$ -maps. The red and blue coloring indicate when  $\gamma > 1$  and identify overestimated dose ( $D_{AAA} > D_{MB}$ ) or underestimated dose ( $D_{AAA} < D_{MB}$ ), respectively.

### Quantification of the impact on dose volume histogram (DVH) metrics

The Figure 4 shows the cumulative and differential DVH from MB and AAA. It takes account of the electrons transport in lateral directions, which causes a decrease of dose for all parameters evaluated in this study. The simulated 95% CIs with bootstrap for  $\Delta D_{min}$ ,  $\Delta D_{mean}$ ,  $\Delta D_{95}$  and  $\Delta D_{max}$  in percentage were, respectively, [7.3; 10.1], [1.5; 2.2], [5.5; 8.2] and [1.0; 3.0]. The Wilcoxon test showed a significant difference with  $P < 0.01$ , except for the maximum dose. The Figure 5 shows the correlation matrix for DVH metrics obtained from MB and AAA.

The 95% CIs for  $CI_{TV}$  were respectively [0.91; 0.97] and [0.7; 0.8] using MB and AAA, with  $P < 0.01$ . The 95% CIs for  $C_{OI}$  were respectively [0.8; 0.9] and [0.7; 0.8] using MB and AAA, with  $P < 0.01$ . Similarly, AAA was predicting more heterogeneous dose in the target predicting more values for S-index. Thus, the 95% CIs for S-index were [1.2; 2.9] using MB method and [2.4; 4.1] using AAA method, with  $P < 0.01$ .

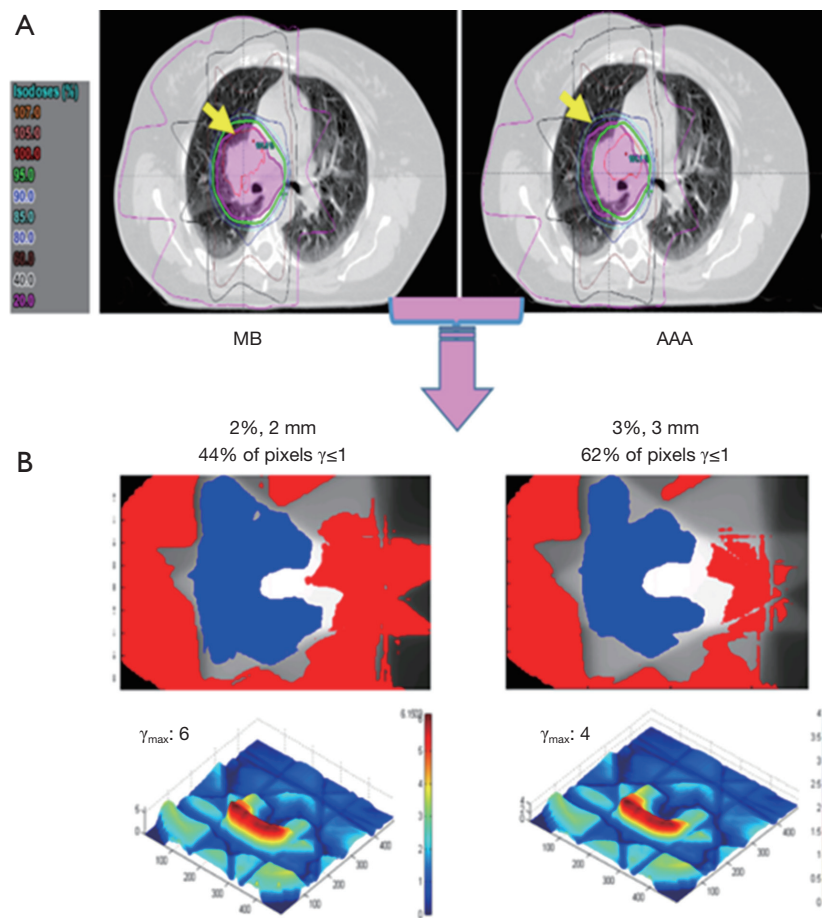


**Figure 3** Dose distribution from MB and AAA for the same patient and same CT-scan. (A) Shows 2D dose maps, the target is presented in violet and the reference isodose curve presented in green; (B) shows 2D  $\gamma$ -map plotted in the axial plan. MB, Modified Batho; AAA, anisotropic analytical algorithm.

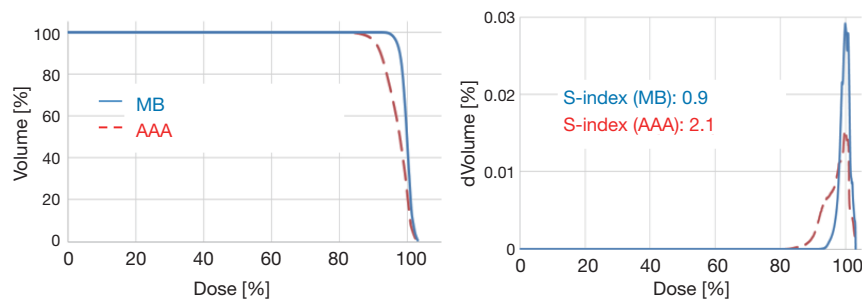


**Figure 4** Cumulative and differential dose volume histograms, respectively on left and right panels calculated using MB-1D density correction and AAA. MB, Modified Batho; AAA, anisotropic analytical algorithm.

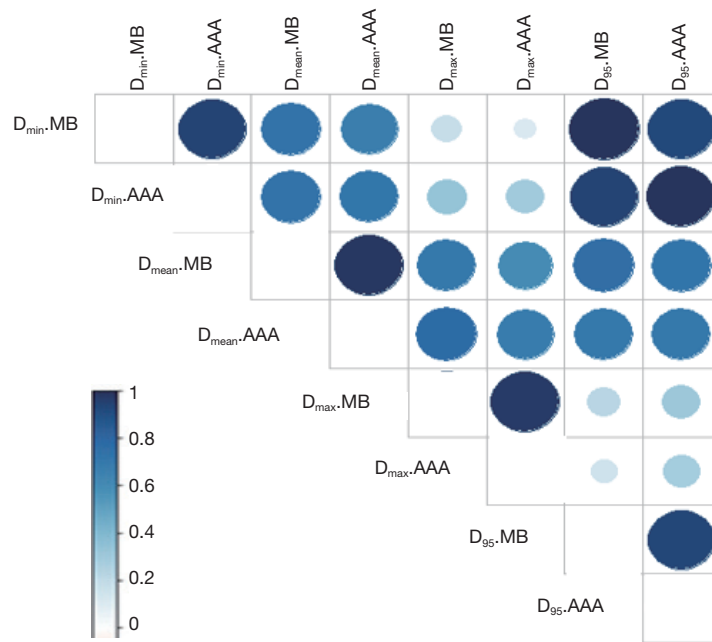


**Figure 5** Correlation matrix for the DVH metrics from MB and AAA. The bar represent the Spearman's rank correlation coefficient value ( $\rho$ ). DVH, dose volume histogram; MB, Modified Batho; AAA, anisotropic analytical algorithm.

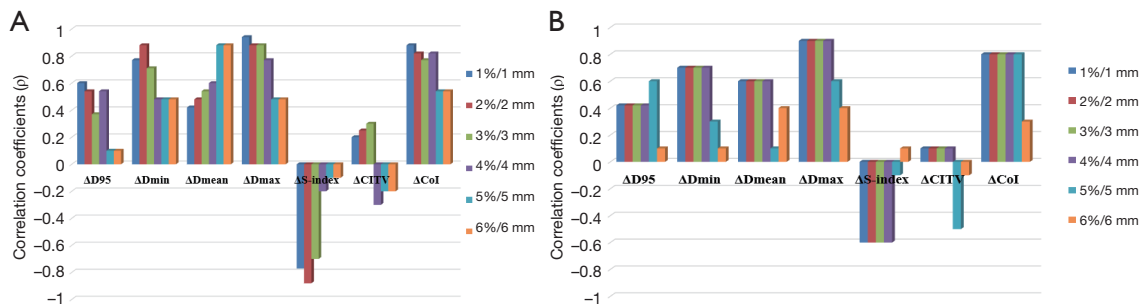


**Figure 6** Correlation between  $\gamma_{rates}$  or  $\gamma_{mean}$  and  $\Delta DVH$  metrics from Eq. [1]. (A) Correlation between  $\gamma_{rates}$  and  $\Delta DVH$  metrics; (B) correlation between  $\gamma_{mean}$  and  $\Delta DVH$  metrics. DVH, dose volume histogram.

**Correlation between  $\gamma$ -index and  $\Delta DVH$  metrics**

The *Figure 6* shows the correlation coefficients ( $\rho$ ) obtained from Spearman's test for  $\gamma_{rates}$  or  $\gamma_{mean}$  with  $\Delta DVH$  metrics. A good correlation between  $\gamma_{rates}$ , resulting from 1%/1, 2%/2 or 3%/3 mm, with  $\Delta D_{min}$ ,  $\Delta D_{max}$  and  $\Delta C_{oI}$ , can be seen. A similar correlation between  $\gamma_{mean}$  and  $\Delta DVH$  metrics was also observed.

**Discussion**

Numerous studies have evaluated the impact of dose

calculation algorithms on dosimetric data for lung irradiations using 1D or 3D methods, equivalent tissue air ratio, AAA, Acuros XB and the most accurate Monte Carlo (MC) algorithm (18,20-25). They reported that the most accurate dose calculation algorithms had a significant impact on DVH metrics and radiobiological indices.

However, this study highlights the discrepancies which can be observed when estimating the dose, in the same patient, taking account or not of the electrons transport, respectively with AAA or MB. This is the first study, which evaluates the amplitude of this effect on DVH and target

coverage using 2D  $\gamma$ -index. In this context, dose differences were expected, but the magnitudes of the discrepancies are very remarkable and considerable, since the lung density is lower compare to other tissues. MB-1D overestimated the target coverage producing treatment plans looking better. However, this study confirms that using AAA, which models the lateral electron transport, the target coverage and the dosimetric data are degraded, compared to the MB-1D density correction. For example, it can be seen in *Figure 3* that the 95% isodose, presented in green color, does not cover the target at all with AAA. This will affect the target coverage by the reference isodose. The 100% isodose curve, presented in red color, was less extended in lateral direction indicating less maximum dose in the target. This is due to the fact that the dose of the secondary electrons is transported farther through the lung. As a result, this will introduce more heterogeneous dose distribution, explaining the over/under estimated dose compared to former algorithms.

The  $\gamma$  analysis in 2D showed that the difference between MB and AAA could reach up to  $\pm 10\%$ . Therefore, the tolerance level of 95% pixels with  $\gamma \leq 1$  was not respected using the routinely  $\gamma$  tolerance 2%/2 mm or 3%/3 mm for quality assurance. Actually the 6%/6 mm criteria were needed to satisfy the required tolerance. The  $\gamma$ -maps, presented in blue color, confirmed that the dose in the beam entrance in the target would be decreased with AAA compared to MB. In the other hand, the extension of secondary electrons, presented in red color, was increased around the healthy lung and organs at risks. This may introduce higher delivered dose for organs at risks, and, as a result, this will predicted more toxicity for healthy lung.

We strongly advise to ascertain better knowledge about the new algorithms before integrating them in radiation oncology department. The  $\gamma$  approach might be a valuable solution to make a medical decision about the need or not for adjustment of the prescribed dose. However, this study has some limits. The dose calculation algorithm is based on AAA. Currently, more advanced algorithms such as Acuros XB in Eclipse<sup>®</sup> or CCC integrated in Pinnacle<sup>®</sup> (Philips Radiation Oncology Systems, Fitchburg, WI) are available for dose calculations. We compared radiotherapy plans using 18 MV, but the use of 6 MV is preferred to treat the lung cancer due to the significant loss of lateral dose equilibrium for high energy in the low density medium (26). In this context, MC simulation could bring more accurate information about extended lateral range of electrons in low density, and provides a quantitative estimation of lateral

and longitudinal effects. Nevertheless, the computation time with MC method is not fast enough to be clinically integrated within a TPS yet. The 2D gamma method can be used to quantify the dose difference between former algorithms and future MC algorithm. The appropriate  $\gamma$  criteria must be assessed to better estimate the correlation between DVH metrics from MC with  $\gamma$  passing rates.

## Conclusions

In this study, we evaluated the dosimetric effects resulting from the transport of electrons on lung radiotherapy treatment plans. We observed a significant effect on the target coverage and the dosimetric data. We revealed the advantage of gamma analysis to show the spatial information about the local dose difference in the target, and the limitations in the use of DVH parameters in evaluating and comparing treatment plans. Significant differences in the delivered dose and D95 were observed between MB-1D and AAA considering that AAA represents the (almost) true delivered dose. This shows that readjusting the prescribed dose and/or optimizing the protection of the organs at risks should be taken into consideration when using more advanced algorithms in order to obtain the best possible clinical outcome.

## Acknowledgements

None.

## Footnote

*Conflicts of Interest:* The authors have no conflicts of interest to declare.

## References

1. Rana S. Clinical dosimetric impact of Acuros XB and analytical anisotropic algorithm (AAA) on real lung cancer treatment plans: review. *Int J Cancer* 2014;2:02019.
2. Ojala J. The accuracy of the Acuros XB algorithm in external beam radiotherapy – a comprehensive review. *Int J Cancer* 2014;2:020417.
3. Bush K, Gagne IM, Zavgorodni S, Ansbacher W, Beckham W. Dosimetric validation of Acuros XB with Monte Carlo methods for photon dose calculations. *Med Phys* 2011;38:2208-21.
4. Aarup LR, Nahum AE, Zacharitou C, Juhler-Nøttrup T,

- Knöös T, Nyström H, Specht L, Wieslander E, Korreman SS. The effect of different lung densities on the accuracy of various radiotherapy dose calculation methods: implications for tumour coverage. *Radiother Oncol* 2009;91:405-14.
5. Bragg CM, Conway J. Dosimetric verification of the anisotropic analytical algorithm for radiotherapy treatment planning. *Radiother Oncol* 2006;81:315-23.
  6. Ahnesjö A. Collapsed cone convolution of radiant energy for photon dose calculation in heterogeneous media. *Med Phys* 1989;16:577-92.
  7. Vanderstraeten B, Reynaert N, Paelinck L, Madani I, De Wagter C, De Gerssem W, De Neve W, Thierens H. Accuracy of patient dose calculation for lung IMRT: A comparison of Monte Carlo, convolution/superposition, and pencil beam computations. *Med Phys* 2006;33:3149-58.
  8. Task Group No.65, the Radiation Therapy Committee of the American Association of Physicists in Medicine. Tissue inhomogeneity corrections for MV photon beams. Madison, WI: Medical Physics Publishing, 2004.
  9. Batho HF. Lung corrections in cobalt 60 beam therapy. *J Can Assoc Radiol* 1964;15:79-83.
  10. El-Khatib E, Battista JJ. Improved lung dose calculation using tissue-maximum ratios in the Batho correction. *Med Phys* 1984;11:279-86.
  11. Sievinen J, Ulmer W, Kaissl W. AAA Photon Dose Calculation Model in Eclipse. Palo Alto (CA): Varian Medical Systems, 2005. [RAD #7170B].
  12. Gagné IM, Zavgorodni S. Evaluation of the analytical anisotropic algorithm in an extreme water-lung interface phantom using Monte Carlo dose calculations. *J Appl Clin Med Phys* 2006;8:33-46.
  13. Low DA, Harms WB, Mutic S, Purdy JA. A technique for the quantitative evaluation of dose distributions. *Med Phys* 1998;25:656-61.
  14. Spezi E, Lewis DG. Gamma histograms for radiotherapy plan evaluation. *Radiother Oncol* 2006;79:224-30.
  15. Chaikh A, Giraud JY, Balosso J. A 3D quantitative evaluation for assessing the changes of treatment planning system and irradiation techniques in radiotherapy. *Int J Cancer* 2014;2:02033.
  16. Yoon M, Park SY, Shin D, Lee SB, Pyo HR, Kim DY, Cho KH. A new homogeneity index based on statistical analysis of the dose-volume histogram. *J Appl Clin Med Phys* 2007;8:9-17.
  17. Feuvret L, Noël G, Mazeron JJ, Bey P. Conformity index: a review. *Int J Radiat Oncol Biol Phys* 2006;64:333-42.
  18. Chaikh A, Giraud JY, Balosso J. A method to quantify and assess the dosimetric and clinical impact resulting from the heterogeneity correction in radiotherapy for lung cancer. *Int J Cancer Ther Oncol* 2014;2:020110.
  19. Chaikh A, Giraud JY, Perrin E, Bresciani JP, Balosso J. The choice of statistical methods for comparisons of dosimetric data in radiotherapy. *Radiat Oncol* 2014;9:205.
  20. Chetty IJ, Devpura S, Liu D, Chen D, Li H, Wen NW, Kumar S, Fraser C, Siddiqui MS, Ajlouni M, Movsas B. Correlation of dose computed using different algorithms with local control following stereotactic ablative radiotherapy (SABR)-based treatment of non-small-cell lung cancer. *Radiother Oncol* 2013;109:498-504.
  21. Liu MB, Eclow NC, Trakul N, Murphy J, Diehn M, Le QT, Dieterich S, Maxim PG, Loo BW Jr. Clinical impact of dose overestimation by effective path length calculation in stereotactic ablative radiation therapy of lung tumors. *Pract Radiat Oncol* 2013;3:294-300.
  22. Hedin E, Bäck A. Influence of different dose calculation algorithms on the estimate of NTCP for lung complications. *J Appl Clin Med Phys* 2013;14:127-39.
  23. Chandrasekaran M, Panettieri V, Baker C, Nahum AE. The clinical impact of differences in photon dose algorithms: 3DCRT and SBRT of lung tumors. *Radiother Oncol* 2011;99:S427-S428.
  24. Huang BT, Lu JY, Lin PX, Chen JZ, Li DR, Chen CZ. Radiobiological modeling analysis of the optimal fraction scheme in patients with peripheral non-small cell lung cancer undergoing stereotactic body radiotherapy. *Sci Rep* 2015;5:18010.
  25. Chaikh A, Giraud JY, Balosso J. Clinical comparison of density correction methods associated with Pencil Beam Convolution algorithm for clinical situations. *Medical physics international Journal* 2014;1:49-53.
  26. Wang L, Yorke E, Desobry G, Chui CS. Dosimetric advantage of using 6 MV over 15 MV photons in conformal therapy of lung cancer: Monte Carlo studies in patient geometries. *J Appl Clin Med Phys* 2002;3:51-9.

**Cite this article as:** Chaikh A, Balosso J. Quantitative comparison of dose distribution in radiotherapy plans using 2D gamma maps and X-ray computed tomography. *Quant Imaging Med Surg* 2016;6(3):243-249. doi: 10.21037/qims.2016.06.04